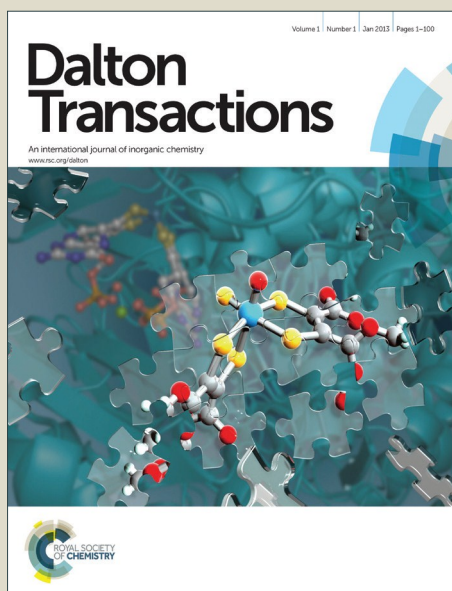


Dalton Transactions

Accepted Manuscript



This article can be cited before page numbers have been issued, to do this please use: I. Romero, M. Rodríguez, I. Ferrer and X. Fontrodona, *Dalton Trans.*, 2016, DOI: 10.1039/C5DT04376J.



This is an *Accepted Manuscript*, which has been through the Royal Society of Chemistry peer review process and has been accepted for publication.

Accepted Manuscripts are published online shortly after acceptance, before technical editing, formatting and proof reading. Using this free service, authors can make their results available to the community, in citable form, before we publish the edited article. We will replace this *Accepted Manuscript* with the edited and formatted *Advance Article* as soon as it is available.

You can find more information about *Accepted Manuscripts* in the [Information for Authors](#).

Please note that technical editing may introduce minor changes to the text and/or graphics, which may alter content. The journal's standard [Terms & Conditions](#) and the [Ethical guidelines](#) still apply. In no event shall the Royal Society of Chemistry be held responsible for any errors or omissions in this *Accepted Manuscript* or any consequences arising from the use of any information it contains.

Ru(II)-dmsO Complexes containing Azole-based Ligands: Synthesis, Linkage Isomerism and Catalytic Behaviour

Íngrid Ferrer, Xavier Fontrodona, Montserrat Rodríguez* and Isabel Romero*

Departament de Química and Serveis Tècnics de Recerca, Universitat de Girona, Campus de Montilivi, E-17071 Girona, Spain.

Abstract

Reaction of *cis, fac*-[RuCl₂(dmsO-S)₃(dmsO-O)], **1**, with different azole (L) ligands leads to new [RuCl₂(L)(dmsO-S)₃] compounds (L = CH₃-pz-H, **2**; NO₂-pz-H, **3**; CF₃-pz-H, **4** and Br-Hind, **5**). Complexes **2-5** have been characterized by analytical, spectroscopic and electrochemical techniques as well as by monocrystal X-ray diffraction analysis. Upon oxidation to Ru(III) the complexes undergo linkage isomerization of a S-bound dmsO ligand and the corresponding kinetic rates as well as the thermodynamic properties have been determined for compound **2** and also for the previously described [Ru^{II}Cl₂(pypz-H)(dmsO-S)₂] (pypz-H = 2-(3-pyrazolyl)pyridine), **6**, from cyclic voltammograms performed at different scan rates. Exposure of compound **2** to visible light in acetonitrile produces a substitution of one dmsO ligand by a solvent molecule generating a new compound, **2'**. The irradiation of solutions of compounds **2** and **6** in chloroform leads in both cases to the substitution of one dmsO by a chlorido ligand in parallel to the oxidation of Ru(II) to Ru(III) generating complexes **2''** and **6'** respectively. The reactivity of compounds **2-6** has been tested with regard to the hydration of nitriles in water as solvent, displaying in all cases good performance and selectivity for the corresponding amides.

KEYWORDS: ruthenium /dmsO complexes/ azole-based ligands / linkage isomerism / hydration catalysis.

Introduction

Ruthenium compounds containing dmsO ligands combined with a variety of auxiliary ligands have been described as potent antitumoral compounds,¹ as precursors for the synthesis of a large variety of complexes² and also as catalysts for a variety of reactions including hydrogen-atom transfer and hydrogenation,³ aerobic oxidation of alcohols,⁴ oxidation of sulphides to sulfoxides⁵ and polymerization of olefins.⁶

The hydration of nitriles to generate the corresponding amides is an important transformation from both academic and industrial point of view.⁷ This reaction is also of biotechnological interest since nitrile hydratases, a family of non-heme iron enzymes,⁸ are used in the industrial preparation of relevant amides such as acrylamide, nicotinamide and 5-cyanovaleramide.⁹ Amides not only constitute versatile building blocks in synthetic organic chemistry¹⁰ but also exhibit a wide range of industrial applications of pharmacological interest.^{9a,11}

The development of new transition metal catalysts able to promote this hydration process under mild conditions and the study of their mechanism is a challenge of special relevance. Most nitrile hydration catalysts proceed by coordinating the nitrile to the metal centre thus activating the former toward nucleophilic attack by water or hydroxyl.¹² The vacant coordination site for coordination of the nitrile would be generated by the dissociation of a labile ligand. Cadierno and others¹³ have developed excellent hydration protocols in pure water under neutral conditions using arene-ruthenium (II) and bis(allyl)-ruthenium (IV) complexes containing P-donor ligands as catalysts. However, to the best of our knowledge, scarce reports on complexes with N- or S-donor ligands applied to hydration of nitriles in water can be found in the literature. We described in a previous work¹⁴ the catalytic hydration activity of the bis-(dmsO-S) Ru complex $[\text{RuCl}_2(\text{pypz-H})_2(\text{dmsO-S})_2]$ (where pypz-H is the bidentate 2-(3-pyrazolyl)pyridine) that displayed good degrees of conversion and selectivity in the hydration of several nitrile substrates, and for which the improved nitrile activation could be related to the remarkable electron-withdrawing character of the dmsO ligands that would accelerate the nucleophilic attack on the Ru-coordinated nitrile substrate. Also, the lability of the dmsO ligands facilitates the generation of vacant coordination sites for the catalytic activity.

On the other hand, dmsO ligand is classified as a versatile molecule because of its ambidentate behaviour and ruthenium compounds containing dmsO ligands have shown to undergo rapid photoinduced and electron-transfer-induced Ru-S/Ru-O linkage isomerism.¹⁵ These properties are crucial to their potential application as optical memory tools,¹⁶ molecular machines¹⁷ and information storage devices.¹⁸ The linkage isomerization has been analysed in detail in Ru(II) complexes containing one or two dmsO ligands^{3,5,15a,19} but, to the best of our knowledge,

no report on such process for Ru(II) complexes with three dmsO ligands has been described. An improved catalytic activity can be expected in these tris-dmsO complexes thanks to the presence of additional π -acceptor dmsO ligands.

In this work we present the preparation and exhaustive characterization of new Ru-(dmsO-S)₃ complexes containing monodentate azole ligands (Scheme 1). We have studied the electron-transfer-induced dmsO-S/dmsO-O linkage isomerization of dmsO ligands in compounds [Ru^{II}Cl₂(CH₃-pz-H)(dmsO-S)₃], **2**, and the bis-dmsO complex [Ru^{II}Cl₂(pypz-H)(dmsO-S)₂], **6**.¹⁴ We also report the reactivity of both compounds towards light irradiation in CHCl₃ and CH₃CN, and the behaviour of the whole family of [RuCl₂(L)(dmsO-S)₃] complexes (where L = pyrazolyl ligands) as catalysts in the hydration of benzonitrile and acrylonitrile in water medium.

Results and discussion

Synthesis and Structure

Reaction of equimolecular amounts of *cis, fac*-[RuCl₂(dmsO-S)₃(dmsO-O)], **1**, and R-pz-H (R= CH₃-, **2**; NO₂⁻, **3**; CF₃⁻, **4**) or Br-Hind (**5**) ligands in refluxing dichloromethane in the absence of light, results in the substitution of the O-bound dmsO ligand in **1** by the corresponding pyrazolyl ligand leading to the formation of the *cis*-Cl, *fac*-dmsO complexes **2-5** (see Scheme 1). The octahedral arrangement of six monodentate ligands in compounds **2-5** can potentially lead to the three isomers depicted in Scheme 2.

It is remarkable that, for compounds **2-4**, we have detected the *cis*-Cl *fac*-dmsO-S (a) as single geometrical isomer either when the reflux time is limited to 1h or extended up to 20h. The preferential formation of the *cis*-Cl *fac*-dmsO-S isomer in these complexes can be rationalized taking into account electronic factors as the synergistic π -donor and π -acceptor effects between the Cl and dmsO ligands mutually placed in *trans*: in the *cis*-Cl *fac*-dmsO-S isomers, two of such Cl-Ru-dmsO-S axes can be found whereas only one or none is present in the rest of isomers. Moreover, in (b) and (c) isomers, two π -donor (Cl) or π -acceptor (dmsO) ligands are necessarily placed in *trans*, which presumably disfavours their formation. For compound **5**, the *cis*-Cl *fac*-dmsO-S isomer (a) is initially formed but a second isomer is detected when the reflux time is extended for longer than 20 minutes. This minor isomer has not been isolated but its resonances are consistent with the (c) ligands disposition (Scheme 2) because it settles a *trans* Cl-Ru-dmsO-S axis in contrast to the more disfavoured Cl-Ru-Cl *trans* disposition in (b). The (c) isomer could be partially favoured in complex **5** thanks to the higher π -acceptor character of the Br-Hind ligand that promotes its coordination in *trans* to a chlorido π -donor ligand.

The crystal structures of complexes **2-5** have been solved by X-ray diffraction analysis. Figure 1 displays their molecular structures whereas selected bond parameters as well as the main crystallographic data can be found in Table 1 and Table S1 (Supporting information) respectively.

In all cases, the Ru metal centres adopt an octahedrally distorted type of coordination with the corresponding pyrazolyl ligand coordinated in *trans* with respect to a dmsO ligand, thus confirming the formation of the (a) isomer as discussed above (Scheme 2). All bond distances and angles are within the expected values for this type of complexes.^{1e,14,19} The four complexes form intramolecular hydrogen bonds between the pyrazole H atoms and the oxygen atom from the *cis* dmsO ligands (H-bond distances are $H_{pz}-O_{dmsO} = 2.012 \text{ \AA}$, **2**; 2.120 \AA , **3**; 1.891 \AA , **4**; 1.952 \AA , **5**). These H-bond interactions are in most cases stronger than the analogous H-bonds found in other complexes containing chelate pyrazolyl ligands, due to the lower geometrical restrictions of the R-pz-H or Br-Hind monodentate ligands with respect to polydentate ligands.^{3,14,19}

Spectroscopic properties

The IR spectra for complexes **2-5** show a band around 1092 cm^{-1} that can be assigned to ν_{S-O} stretching of sulphur-coordinated dmsO ligands as S-coordination increases the S-O bond order in the dmsO molecule, thus shifting the corresponding ν_{S-O} stretch frequency to values above that of free dmsO (1050 cm^{-1}). This is also corroborated by the absence of any S-O stretching vibration in the $920-930 \text{ cm}^{-1}$ range, which would conversely indicate O-coordinated dmsO ligands.^{2a}

The one dimensional (1D) and two-dimensional (2D) NMR spectra of complexes **2-5** were registered in CD_2Cl_2 and are presented in the Supplementary Information (Figures S1-S4). The resonances found for all the complexes are consistent with the structures obtained in the solid state. The complexes exhibit two sets of signals: one in the aromatic region corresponding to the nitrogen ligands and the other one in the aliphatic region with three singlets corresponding to the methyl groups of the bonded dmsO ligands (and an additional singlet assigned to the pyrazole methyl group in the case of complex **2**). The complexes display a symmetry plane that contains the pyrazolyl ligand and the dmsO in *trans* to it and thus the two methyl groups of this *trans* dmsO (for instance C8 and C7 in complex **2**, see Figure 1) are magnetically equivalent. The two remaining dmsO show two additional singlets that, from symmetry considerations, can be tentatively assigned (in the case of complex **2**) to C5+C10 ($\delta = 3.40 \text{ ppm}$) and C6+C9 ($\delta = 3.12 \text{ ppm}$), on the basis of the deshielding effect produced by the two Cl ligands, closer to C5 and C10. The NOE crosspeaks observed between the pyrazolic hydrogen H2 and the singlets at 3.12 and 3.40 ppm (taking

complex **2** as example) allows identifying unambiguously the two dmsos in *cis* to the pyrazolyl ligand. The intramolecular hydrogen bonds observed in the structure of these complexes have been also evidenced in solution because the pyrazolic hydrogen atoms appear downfield in all cases with respect to the corresponding free ligands, and are also more deshielded than the rest of the hydrogen atoms upon coordination.

The UV-Vis spectra of complexes **2-5** are displayed in the Supplementary Information (Figure S5) and the spectral features of complexes are presented in the experimental section. The complexes exhibit ligand based π - π^* bands below 300 nm and relatively intense bands above 300 nm mainly due to $d\pi$ - π^* MLCT transitions.²⁰ The low aromatic character of the pyrazole ring involves ligand orbitals of relatively high energy thus leading to the occurrence of $d\pi$ - π^* absorptions at lower wavelengths than those of analogous complexes containing pyridylpyrazole ligands, with aromatic pyridine rings directly bound to the metal,^{3,14} and also increases the π - π^* absorption energies that in some cases appear out of the solvent range.

Redox chemistry and linkage isomerization

The redox properties of complexes **2-5** have been investigated by cyclic voltammetry (CV) experiments, and the voltammogram of **2** in acetonitrile, starting at 0 V at a scan rate of 0.1 V, is shown in Figure 2 (solid line). As can be observed an anodic wave, corresponding to the oxidation of the $\text{Ru}^{\text{II}}(\text{dmsos})$ species to $\text{Ru}^{\text{III}}(\text{dmsos})$, is observed at $E_{pa} = 1.49$ V vs Ag/AgCl. This redox process is irreversible and this behaviour can be attributed to a relatively fast linkage isomerization of a dmsos ligand in the oxidized species forming $\text{Ru}^{\text{III}}(\text{dmsos})$ (see Scheme 3), as will be discussed below. Oxygen-coordinated dmsos is a favoured form in Ru(III) complexes, consistently with Pearson's concept of hard and soft acids and bases for the harder Ru(III) Lewis acid. Upon back scanning to negative potential a cathodic peak at $E_{pc} = 0.75$ V is observed which is consistent with the reduction of the isomerized species to form $\text{Ru}^{\text{II}}(\text{dmsos})$ that, after reduction, would rearrange to restore the initial complex. This process becomes more evident by starting the scan at the highest potential value (1.8 V) and applying an initial equilibration time of 10 min (Figure 2, dashed line). Under these conditions the anodic peak corresponding to the oxidation of $\text{Ru}^{\text{II}}(\text{dmsos})$ to $\text{Ru}^{\text{III}}(\text{dmsos})$ can be observed, and an additional reversible wave a $E_{1/2} = 0.98$ V appears, corresponding probably to the substitution of one dmsos by acetonitrile solvent.

Complexes **3-5** display identical behaviour to that described for complex **2** (see Figure S6), whereas the pypz-H complex **6** also undergoes a dmsos linkage isomerization process, though it is not complete on the scale time of the

cyclic voltammetry (see below). The electrochemical data for all the complexes together with those of the pyrazole compound $[\text{Ru}^{\text{II}}\text{Cl}_2(\text{pz-H})(\text{dmsO-S})_3]$ are gathered in Table 2. In all cases, potential shifts of 0.7-0.9 V are observed between the E_{pa} ($\text{Ru}^{\text{II}}\text{-S}\rightarrow\text{Ru}^{\text{III}}\text{-S}$) and E_{pc} ($\text{Ru}^{\text{III}}\text{-O}\rightarrow\text{Ru}^{\text{II}}\text{-O}$) values, due to the lower electron-withdrawing ability of the O-coordinated dmsO that makes the upper oxidation states of Ru more accessible. These shift values are in the same range as those observed in complexes where the isomerization of only one dmsO ligand takes place,^{3,19} then suggesting that this is also the case for complexes **2-6**.

The redox potential values for these compounds are consistent with the electronic characteristics of the substituents on the pyrazole ligands. Thus compound **2**, containing a methyl σ -donor substituent, presents lower E_{pa} values than compounds $[\text{Ru}^{\text{II}}\text{Cl}_2(\text{pz-H})(\text{dmsO-S})_3]$ ¹⁴ and **3-5**, the latter containing π -acceptor substituents. However, the effect of the π -acceptor substituents on the potential values is clearly stronger in complex **4**, containing a $-\text{CF}_3$ substituent. This fact could probably be due to the more extensive electronic delocalization of the $-\text{NO}_2$ and $-\text{Ph}$ substituents over the pyrazolic ring in **3** and **5**, which would presumably lead to a weaker π -acceptor character of these ligands and therefore to an only moderate increase of the E_{pa} value in comparison to the pz-H complex. In the case of compound $\text{Ru}^{\text{II}}\text{Cl}_2(\text{pypz-H})(\text{dmsO-S})_2$ **6**,¹⁴ containing the bidentate pyridine-pyrazole ligand, a formal substitution of one dmsO ligand by a pyridine ring takes place and this shifts the E_{pa} ($\text{Ru}^{\text{II}}\text{-S}\rightarrow\text{Ru}^{\text{III}}\text{-S}$) to significantly lower values ($E_{1/2}=1.09$ V) when compared to the whole series of tris-dmsO complexes, thus manifesting the higher π -acceptor capacity of dmsO ligands with respect to a pyridine ring.

A throughout kinetic study has been carried out on the linkage isomerization experimented by complexes **2** and **6**, following the method described in the literature by Nicholson and Shain²¹ that is detailed step by step below.

The scan rates directly influence the intensity of waves of the cyclic voltammograms and this dependence provides information about the participation of chemical reactions coupled to electrochemical processes (as is the example of dmsO linkage isomerization shown in Scheme 3), allowing the determination of the corresponding rates and equilibrium constants. We have calculated these constants for the dmsO linkage isomerization on compounds **2** and **6** both containing pyrazolyl type of ligands. To do so, cyclic voltammetries at different scan rates, starting the potential scanning from the lower and upper points of the CV range, have been registered for both complexes in CH_2Cl_2 (chosen as solvent with the idea to avoid ligand solvolysis). The set of formulas used are gathered in the Supplementary Information (Table S3) and the results obtained are gathered in Table 3 together with other Ru complexes described in the literature.

The equilibrium constants for the $\text{Ru}^{\text{III}}\text{-O} \rightleftharpoons \text{Ru}^{\text{III}}\text{-S}$ reaction ($K^{\text{III}}_{\text{O-S}}$) can be obtained in each case from cyclic voltammograms recorded through starting the potential scanning from the upper E_{init} values (1.7 V for **2** and 1.4 V for **6** with 1 minute of equilibration time at the initial potential in both cases, see Figure 3) and applying equation 1 (Table S3). Plotting the ratio $i_{\text{c1}}/i_{\text{c2}}$ vs v^{-1} and extrapolating v to infinite in order to obtain the intercept values (Figures S8 and S9) results in $K^{\text{III}}_{\text{O-S}} = 0.036$ for **2** and $K^{\text{III}}_{\text{O-S}} = 1.39$ for **6** (see Table 3).

The kinetic isomerization constants ($k^{\text{III}}_{\text{O-S}}$ and $k^{\text{III}}_{\text{S-O}}$) are calculated from plotting $v^{1/2}$ vs. the $i_{\text{d}}/i_{\text{k}}$ ratio (eq. 2, Table S3), where i_{k} represents the measured peak current (i_{c1}) and the i_{d} the corresponding diffusional current in the absence of a chemical reaction (i_{a1}). The i_{k} and i_{d} values were obtained respectively from the cyclic voltammograms registered through reverse (Figure 3) and direct (Figure S7) scan potential. From the value of slope obtained (Figures S10 and S11), and considering that $K^{\text{III}}_{\text{O-S}} = k^{\text{III}}_{\text{O-S}}/k^{\text{III}}_{\text{S-O}}$, the following kinetic constants can be calculated: for complex **2**, $k^{\text{III}}_{\text{O-S}} = 0.019 \text{ s}^{-1}$ and $k^{\text{III}}_{\text{S-O}} = 0.53 \text{ s}^{-1}$; for complex **6**, $k^{\text{III}}_{\text{O-S}} = 0.176 \text{ s}^{-1}$ and $k^{\text{III}}_{\text{S-O}} = 0.126 \text{ s}^{-1}$.

With the equilibrium constant $K^{\text{III}}_{\text{O-S}}$ and assuming that $E^{\circ} = E_{1/2}$ or E_{pa} for each linkage isomer, equation 3 (Table S3) can be used to calculate the equilibrium constant for the $\text{Ru}^{\text{II}}\text{-O} \rightleftharpoons \text{Ru}^{\text{II}}\text{-S}$ process in the Ru(II) oxidation state, $K^{\text{II}}_{\text{O-S}}$, resulting in $K^{\text{II}}_{\text{O-S}} = 1.53 \cdot 10^{12}$ for **2** and $K^{\text{II}}_{\text{O-S}} = 1.34 \cdot 10^{12}$ for **6**. Finally, the kinetic isomerization constants in the Ru(II) oxidation state can be calculated from eq. 4 in Table S3²² and the linear fit of the corresponding plots (Figures S12 and S13) yield $k^{\text{II}}_{\text{O-S}} = 0.072 \text{ s}^{-1}$ and $k^{\text{II}}_{\text{S-O}} = 4.7 \cdot 10^{-14} \text{ s}^{-1}$ for **2** and $k^{\text{II}}_{\text{O-S}} = 0.11 \text{ s}^{-1}$ and $k^{\text{II}}_{\text{S-O}} = 8.2 \cdot 10^{-14} \text{ s}^{-1}$ for **6**.

The high values of $K^{\text{II}}_{\text{O-S}}$ obtained for compounds **2** and **6** (see Table 3) indicate that, in Ru(II) redox state, the dmsO ligand displays a high preference to be bound to the metal through the S atom in both cases, and the thermodynamic stability of this form is slightly higher in **2** than in **6**. The major stability of complex **6** in the Ru(II) state with regard to the structurally similar compounds of entries 3-5 in Table 3 is not easy to explain but could be related to the distinctive electronic characteristics and the higher volume of the H3p and bpp ligands when compared to pypz-H. Also, in complexes *trans,cis*-[RuCl₂(H3p)(dmsO-S)₂] and *trans,cis*-[RuCl₂(bpp)(dmsO-S)₂] (entries 4 and 5) the *trans* disposition of the two chlorido ligands probably diminishes the overall electron density on the Ru metal centre then facilitating the Ru-S → Ru-O isomerization. A similar argument would explain the lower relative stability of complex *out*-[Ru(L²)(trpy)(dmsO-S)]⁺ (entry 6) where only one anionic ligand (the deprotonated L²) is present.

In the Ru(III) state, linkage isomerization takes place in both complexes (as evidenced by the cyclic voltammograms discussed above) but, as can be inferred from K_{O-S}^{III} values, the Ru-S bound form is still dominant for complex **6** whereas complex **2** presents a marked preference for the Ru^{III}-O isomer, which is one or two orders of magnitude higher than the rest of the complexes in Table 3. This is in accordance with the CVs registered for both complexes, where the cathodic peak corresponding to the Ru^{III}-S → Ru^{II}-S reduction process is observed only for complex **6** whilst complex **2** displays a complete isomerization towards the Ru-O form immediately after Ru(II) → Ru(III) oxidation. Steric factors could be responsible for the higher stability of the isomerized form in **2** since three S-bound dmsoligands would probably encounter significant steric hindrance when coordinating in facial arrangement the smaller Ru(III) ion.

Complex **2** also presents a higher k_{S-O}^{III} kinetic constant than **6** and this could be due to the presence of an additional S-bound dmsoligand in **2** instead of the pyridyl ring in **6**. A larger number of highly π -acceptor auxiliary ligands will presumably increase the Ru-S → Ru-O isomerization rate upon Ru(II) → Ru(III) oxidation, and this is in accordance with complex *out*-[Ru(L²)(trpy)(dmsol-S)]⁺ (entry 6) being the one with the largest k_{S-O}^{III} value as it contains four π -acceptor pyridyl ligands and only one anionic pyrazolate ring coordinated to Ru. However, it is noticeable that complex **2**, in spite of bearing two anionic π -donor Cl ligands, presents a k_{S-O}^{III} value comparable to that found for the complex in entry 6, then evidencing the remarkable influence exerted by the third dmsoligand over the isomerization process in **2**. Steric factors arising from the aforementioned facial coordination of three bulky dmsoligands might also hasten the linkage isomerization in this case. The high kinetic rates for the Ru^{III}-S → Ru^{III}-O process in **2** and *out*-[Ru(L²)(trpy)(dmsol-S)]⁺ are also consistent with the practically quantitative isomerization observed experimentally for both complexes.⁵

Photoinduced substitution reactions

In a previous work¹⁴ we have investigated the photochemical behaviour of compound **6** in a coordinating solvent as acetonitrile evidencing the occurrence of light-induced processes where the substitution of one dmsoligand by acetonitrile took place. On the other hand, photoinduced decomposition of CHCl₃ in presence of Ru(II) compounds has been also described in the literature.²³ In this context, and in order to obtain information about the lability of the ligands in the synthesized complexes given their potential involvement in some catalytic processes, we have studied the behaviour of compounds **2** and **6** in CHCl₃ and that of complex **2** in CH₃CN in presence of light (Scheme 4).

On irradiating a 1 mM solution of **2** in acetonitrile with an 80W lamp, the colour of the solution changes from pale to deep yellow, indicating the occurrence of light-induced processes. The changes have been monitored through UV-vis, NMR and cyclic voltammetry experiments.

The UV-vis spectra registered during 90 minutes (Figure 4) show two isosbestic points at 327 and 403 nm and a new MLCT band appears a higher wavelength (432 nm), which would be consistent with the substitution of a dmsO ligand by a less π -acceptor acetonitrile ligand (leading to the formation of the new compound $[\text{RuCl}_2(\text{MeCN})(\text{CH}_3\text{-pz-H})(\text{dmsO-S})_2]$, **2'**) but could also indicate a geometrical rearrangement from a *cis*-Cl to a *trans*-Cl geometry of complex **2**, as has been reported for other dihalide Ru-dmsO complexes.^{2b,c} Ligand substitution by acetonitrile is evidenced by NMR and cyclic voltammetry experiments (see below), but simultaneous structural reorganization cannot be ruled out. Keeping the irradiation for longer led to the disappearance of the isosbestic points, consequently indicating that multiple light-induced processes must be taking place.

The changes in the ¹H-NMR spectrum of the aliphatic region upon **2**→**2'** photochemical substitution (Figure S14) clearly show that free dmsO (δ 2.6 ppm) is progressively generated along with the disappearance of the three dmsO singlets located at 3.40, 3.36 and 3.1 ppm. Two new resonances with equal integration values appear at 3.04 and 3.26 ppm that are also consistent with the generation of the bis-dmsO compound **2'** where two types of magnetically equivalent $\text{CH}_3(\text{dmsO})$ groups are present. These NMR spectra would be consistent with the generation of either *cis*-Cl or *trans*-Cl $[\text{RuCl}_2(\text{MeCN})(\text{CH}_3\text{-pz-H})(\text{dmsO-S})_2]$.

The substitution process in **2** has also been followed through cyclic voltammetry (CV) experiments (see Figure S15). The intensity of the initial redox wave at $E_{\text{pa}}=1.49$ V progressively decreases upon irradiation, in parallel with the appearance of a new reversible wave at $E_{1/2}=1.04$ V. The lower half-potential value for the substituted compound is consistent with the exchange of one dmsO by MeCN since the replacement of an anionic Cl ligand by a neutral MeCN would generate much higher redox potentials.²⁴ The new wave observed around 1.2 V corresponds to the oxidation of free dmsO which is also in accordance with the formation of **2'**.

The substitution process by acetonitrile has been described in the literature with compounds containing one or two dmsO ligands^{3,5,15a,19,25} but, to the best of our knowledge, this is the first Ru(dmsO)₃ compound that presents this behaviour. Unfortunately, all attempts to isolate compound **2'** have failed.

On the other hand, similar experiments were carried out for **2** and **6** in chloroform, chosen as non-coordinating solvent, with the aim to evaluate the photochemical behaviour of the complexes in particular regarding the dmsO

linkage isomerization. However, after irradiating a solution of complex **6** in chloroform for 12 h the solution colour changed from yellow to red-brown. On the basis of similar systems described in the literature,¹⁹ we could unravel that the substitution of one dmsoligand by a chlorido ligand and the subsequent oxidation of Ru(II) to Ru(III) had taken place, leading to the formation of a new complex, *mer*-[Ru^{III}Cl₃(pypz-H)(dmsol-S)] (**6'**). The light-induced reaction of Ru(II) complexes with CHCl₃ has already been described and seems to be initiated by high-energy transitions of the complex.¹⁹

The new complex **6'** was isolated by precipitation with ether, and suitable crystals for X-ray diffraction analysis were obtained. The corresponding ORTEP plot is shown in Figure 5, where it can be observed that the complex displays a distorted octahedral geometry with a meridional disposition of the three chlorido ligands. The structural features of compound **6'** are similar to other tris-chlorido compounds described in the literature.¹⁹ The main crystallographic data and selected bond distances and angles for the structure can be found in Tables 1 and S1.

It is remarkable that, despite the Ru(II)→Ru(III) oxidation, the remaining dmsoligand in **6'** is coordinated by the sulphur atom so that no linkage isomerization has taken place, probably due to the stabilization of this dmsol by an intramolecular hydrogen bond ($H_{\text{pz}}-\text{O}_{\text{dmsol}} = 2.296 \text{ \AA}$) and also to the weakened Lewis acid character of the metal by the presence of an additional strongly σ -donor chlorido ligand.

The CV registered after irradiation (Figure S16) shows that this substitution provokes a decrease of the Ru(III/II) $E_{1/2}$ value from 1.09 to 0.05 V due to the additional electron-donating ability of the new chlorido ligand. The evolution of the UV-Vis spectra throughout the substitution process is depicted in Figure S17 and the final spectrum, corresponding to **6'**, shows spectral features such as those displayed by other similar compounds described.¹⁹ A shift to lower energy absorptions is observed due to the higher σ and lower π -acceptor capacity of the Cl ligand with regard to dmsol, that provokes a destabilization of the $d\pi(\text{Ru})$ donor orbital. Also, a different pattern of absorption bands was observed with additional $\text{Cl}_{\text{p}\pi}-\text{Ru}_{\text{d}\pi^*}$ LMCT in the visible region.²⁶ Two isosbestic points at 328 and 352 nm are found, confirming the net conversion of **6** into **6'**.

On the other hand, the irradiation of a chloroform solution of compound **2** lead to a colour change from yellow to brown presumably due, as described above for **6**, to a dmsol substitution by chlorido with concomitant oxidation of Ru(II) to Ru(III), generating the new complex $[\text{Ru}^{\text{III}}\text{Cl}_3(\text{CH}_3\text{-pz-H})(\text{dmsol-S})_2]$, **2''**. The UV-Vis spectra registered during 24 hours (Figure S18) show spectral features such as those displayed by other similar compounds described

in the literature¹⁹ and thus the substitution of one dmsO ligand by a chlorido ligand, together with the oxidation of Ru(II) to Ru(III), has seemingly taken place leading to the generation of complex **2''**.

The CV registered after irradiation, starting the potential scanning at -0.2 V vs Ag/AgCl (Figure S19), shows two new redox processes at $E_{1/2} = 0.1$ V and 0.3 V that, unlike the former Ru(III/II) wave in **2**, are electrochemically reversible. We have further investigated the electrochemical behaviour displayed by complex **2''** through differential pulse voltammetry (DPV) at different initial equilibrium times and starting the potential scanning at -0.2 or at +0.6 V. The DPV obtained are displayed in Figure 6 and, as can be observed, the redox process at $E_{1/2} = 0.3$ V is manifested only when the potential scanning starts at low E values (Figure 6a). Moreover, upon lengthening the equilibrium time the relative intensity of this redox process (compared to that at $E_{1/2} = 0.1$ V) increases from approximately 1:1 at equilibrium time = 0 s up to 1:2.5 at equilibrium time = 180 s. The reverse scanning potential (Figure 6b) mainly displays the $E_{1/2} = 0.1$ V redox process independently of the equilibrium time applied. Taking into account these observations a plausible explanation is that the irradiation of **2** leads predominantly to the formation of a Ru(III) complex (**2''**) where one of the two remaining dmsO ligands has undergone linkage isomerization and is bound through its O atom. This Ru-O_{dmsO} compound, that displays a Ru(III/II) redox process at $E_{1/2} = 0.1$ V, experiences a partial Ru-O → Ru-S isomerization upon reduction to Ru(II), generating a new linkage isomer with $E_{1/2} = 0.3$ V where the two dmsO ligands are coordinated through their S atoms.

The behaviour displayed by the Ru(III) tris-chlorido complex **2''** differs from that discussed above for complex **6'**, where the remaining dmsO ligand was coordinated through sulphur despite being a Ru(III) compound. Some factors could explain this distinctive behaviour: 1) as discussed earlier, a dmsO ligand presents higher π -acceptor character than a pyridyl ring and, consequently, the overall electron-withdrawing character of the ligands is enhanced in **2''** when compared to **6'**, thus facilitating the isomerization towards the less π -acceptor O-bound dmsO; 2), the remaining dmsO ligand in **6'** is stabilized by H-bonding interactions with the pyrazolyl H atom.

On the other hand, the difference between the potential values for the O- and S-bound dmsO forms in **2''** (approximately 0.2 V) is lower than that displayed by complexes **2-5** and **6**, which is around 0.6-0.8 V. This could be explained by the increased electron density at the Ru metal centre in **2''** thanks to the third anionic chlorido ligand that probably balances to a higher extent the electron-withdrawing character of a S-bound dmsO. Unfortunately, the isolation of suitable crystals for the X-ray diffraction structure of this species has not been achieved so the presence of an O-bound dmsO cannot be unambiguously confirmed. Yet, the low potential values

observed are in agreement with the substitution of one dmsO by a chlorido ligand owing to the higher electron-donating character of the latter.

Catalytic hydration of nitriles

We have checked the activity of complexes **2-6** as precatalysts in the hydration process of benzonitrile and acrylonitrile as substrates, in neutral conditions using water as solvent at 80°C. The remaining nitrile has been quantified through GC chromatography with biphenyl as internal standard and the hydrolysis products have been analysed by NMR spectroscopy and compared to pure samples of the corresponding amide and acid derivatives. Conversion and selectivity values are summarized in Table 4 together with the results previously obtained for the analogous complex $[\text{RuCl}_2(\text{pz-H})(\text{dmsO-S})_3]$, containing the pyrazole ligand.¹⁴ Blank experiments without any catalyst were carried out by keeping the substrates in water at 80°C for 20h. In all cases, the nitrile was quantitatively recovered.

As we can observe in Table 4, the complexes were found to be active towards nitrile hydration with moderate conversion values (though for benzonitrile hydration with complex **3** a good conversion value of 85% is attained). However, the most remarkable feature is the excellent selectivity observed for the corresponding amides in all cases. It is interesting to emphasize the performance of these compounds in the hydration of acrylonitrile, where the industrially relevant acrylamide product is quantitatively obtained.

A possible mechanism currently accepted in the hydration of nitriles is a ligand substitution process, where a labile ligand is initially replaced by the corresponding nitrile substrate.¹² Then, the electronic properties of the catalysts will likely influence the extent of the hydration reaction, providing that a nucleophilic attack of water (or hydroxo anions) on the nitrile carbon atom takes place.²⁷ The relatively good performance of compounds **2-5** could be explained by electronic factors (a high number of electron-withdrawing ligands that would render the ruthenium metal centre more electrophilic and consequently would lead to a better nitrile activation upon coordination) and also by the occurrence of a large number of potentially labile sites, presumably those occupied by dmsO ligands. Decoordination of dmsO during the catalytic process is supported by the fact that free dmsO is found in all cases when analysing the hydrolysis products by NMR spectroscopy. To further confirm dmsO decoordination, a sample of catalyst **2** was kept in water at 80°C and the evolution was monitored through UV-vis spectroscopy (Figure S20). A new band at 516 nm progressively appears which

would be in accordance with the substitution of a dmsoligand by a less π -acceptor aqua or hydroxo ligands. This is also consistent with the displacement of the ligands resonances observed in the final $^1\text{H-NMR}$ spectrum together with an increase of the free dmsoligand signal (Figure S21). However, the final NMR shows the presence of multiple resonances which can be indicative of the formation of distinctive hydrolysed Ru species.

Clear differences in the conversion values are observed in Table 4 among catalysts **2-5** (containing monodentate pyrazolyl ligands) in the hydration of a specific substrate that are likewise originated by the distinctive electronic characteristics of the monodentate azole ligands, as the rest of ligands and the catalyst geometry are identical for the whole set of complexes **2-5**. This influence can be observed for instance when using benzonitrile as substrate. Indeed, an enhanced performance is found, as expected, for complex **3** having the NO_2 electron-withdrawing substituent when compared to $[\text{RuCl}_2(\text{pz-H})(\text{dmsol-S})_3]$, and a decrease in conversion is shown for the methylpyrazole complex **2**, with a more σ -donor ligand. The indazole complex **5** would also be expected to display better activity than $[\text{RuCl}_2(\text{pz-H})(\text{dmsol-S})_3]$ but this is not the case, probably due to a certain delocalization effect of the π electron density of the Br-phenyl ring on the pyrazole. Complex **4** is also expected to display improved activity, but it undergoes a colour change during the catalytic process that most certainly indicates a catalyst deactivation, thus yielding the lowest conversion value for this substrate. For complex **6**, the formal replacement of a dmsoligand by a pyridyl ring slightly decreases the conversion value with regard to $[\text{RuCl}_2(\text{pz-H})(\text{dmsol-S})_3]$ but still displaying a relatively good performance. Structural factors might also be influencing the performance of complex **6** due to the presence of a more rigid bidentate ligand.

The comparison of catalysts **2-5** in the hydration of acrylonitrile follows a tendency similar to that described above for benzonitrile: complex **2** displays lower activity than $[\text{RuCl}_2(\text{pz-H})(\text{dmsol-S})_3]$ and complex **5** performance is lower than expected. Yet, in this case complex **4**, with the CF_3 substituent, does not undergo any remarkable change of colour that could be related to catalyst decomposition as was the case for benzonitrile, and it displays a relatively high activity. Finally, complex **6** displays low performance for the hydration of acrylonitrile, with only 22% conversion. These results would manifest a certain influence of the electronic characteristics of the substrates as the more electrophilic catalysts **3** and **6** attain relatively good conversion values for the more activated substrate benzonitrile, whereas for acrylonitrile (where electronic factors of the substrate are not expected to have a relevant influence) the performances are moderate.

Conclusions

We have synthesized and fully characterized a new family of Ru(dms_o)₃ complexes containing azole-based ligands. The substituents on the ligands do not have any remarkable influence on the structural parameters but some differences are exhibited in the redox potential values and in the performance of the complexes towards the hydration of nitriles in water. All compounds have displayed good selectivity for the amide products being the first Ru(dms_o)₃ compounds capable to carry out this reaction in water.

Upon oxidation to Ru(III), linkage isomerization of one of the S-coordinated dms_o takes place in the case of compounds **2** and **6**, and scan rate dependent voltammograms permitted to estimate the kinetic linkage isomerization rates and the thermodynamic equilibrium constants evidencing a markedly higher preference of complex **2** for the O-dms_o form in the oxidation state Ru(III) when compared to that of **6**, which is in accordance with the high degree of linkage isomerization found for the former in cyclic voltammetry experiments. The differences observed between both compounds arise from electronic factors promoted by the presence of an additional dms_o ligand in compound **2** with regard to **6**. Exposure of compounds **2** and **6** to visible light in acetonitrile and chloroform produces the substitution of one dms_o ligand by CH₃CN or a chlorido ligand respectively, with a concomitant Ru(II)→Ru(III) oxidation in the latter case.

Experimental Section

Materials

All reagents used in the present work were obtained from Aldrich Chemical Co and were used without further purification. Reagent grade organic solvents were obtained from SDS and high purity de-ionized water was obtained by passing distilled water through a nano-pure Mili-Q water purification system. RuCl₃·2H₂O, was supplied by Johnson and Matthey Ltd. and was used as received.

Instrumentation and Measurements

IR spectra were recorded on an ATR MK-II Golden Gate Single Reflection. UV-Vis spectroscopy was performed on a Cary 50 Scan (Varian) UV-Vis spectrophotometer with 1 cm quartz cells. Cyclic voltammetric (CV) and Differential Pulse Voltammetry (DPV) experiments were performed in an IJ-Cambria IH-660 potentiostat using a three electrode cell. Glassy carbon electrode (3 mm diameter) from BAS was used as working electrode, platinum wire as auxiliary and Ag/AgCl as the reference electrode. All cyclic voltammograms presented in this work were recorded under nitrogen atmosphere. The complexes were dissolved in solvents containing the necessary amount of

n-Bu₄NH⁺PF₆⁻ (TBAH) as supporting electrolyte to yield a 0.1 M ionic strength solution. All $E_{1/2}$ values reported in this work were estimated from cyclic voltammetric experiments as the average of the oxidative and reductive peak potentials ($(E_{pa}+E_{pc})/2$), or directly from DPV. Unless explicitly mentioned the concentration of the complexes was approximately 1mM. The NMR spectroscopy was performed on a Bruker DPX 300 and 400 MHz. Samples were run in CD₂Cl₂ or d₃-acetonitrile with internal references (residual protons and/or tetramethylsilane). Elemental analyses were performed using a CHNS-O Elemental Analyser EA-1108 from Fisons. Monochromatic irradiations were carried out by using a 80 W lamp source from Phillips on complex solutions, typically 1mM. Gas chromatography experiments were performed by capillary GC, using a GC-2010 Gas Chromatograph from Shimadzu, equipped with an Astec CHIRALDEX G-TA Column (30 m x 0.25 mm diameter) incorporating a FID detector. All the product analyses in the catalytic experiments were performed by means of GC using biphenyl as internal standard.

Crystallographic Data Collection and Structure Determination

Measurement of the crystals were performed on a Bruker Smart Apex CCD diffractometer using graphite-monochromated Mo K α radiation ($\lambda = 0.71073\text{\AA}$) from an X-Ray tube. Data collection, Smart V. 5.631 (Bruker AXS 1997-02); data reduction, Saint+ Version 6.36A (Bruker AXS 2001); absorption correction, SADABS version 2.10 (Bruker AXS 2001) and structure solution and refinement, structure solution and refinement, SHELXL-2013 (Sheldrick, 2013). The crystallographic data as well as details of the structure solution and refinement procedures are reported in supplementary information. CCDC 1423204 (**2**), 1423200 (**3**), 1423202 (**4**), 1423201 (**5**) and 1423203 (**6'**) contain the supplementary crystallographic data for this paper. These data can be obtained free of charge from The Cambridge Crystallographic Data Centre via www.ccdc.cam.ac.uk/products/csd/request/

Catalytic studies

The ruthenium catalyst (0.01 mmol), water (3 ml) and the corresponding nitrile (1 mmol) were introduced into a sealed tube and the reaction mixture stirred at 80°C. The nitrile was extracted with chloroform and quantified by GC, whereas the identity and purity of the resulting amides was assessed by ¹H-NMR on the reaction crude.

Preparations

cis, fac-[RuCl₂(dmsO-S)₃(dmsO-O)], **1**,^{2a} and [Ru^{II}Cl₂(pypz-H)(dmsO-S)₂], **6**,¹⁴ complexes were prepared according to literature procedures. All synthetic manipulations were routinely performed under nitrogen atmosphere using vacuum line techniques. Electrochemical experiments were performed under N₂ atmosphere with degassed solvents.

All spectroscopic, electrochemical and synthetic experiments were performed in the absence of light unless explicitly mentioned.

[Ru^{II}Cl₂(CH₃-pz-H)(dmsO-S)₃], 2. A 0.034g (0.414 mmol) sample of fomezazole ligand and *cis, fac*-[RuCl₂(dmsO-S)₃(dmsO-O)] (0.2 g, 0.413 mmol) were dissolved in 10ml of dichloromethane and the resulting solution refluxed for 1 h at 60°C. After this time, the mixture was allowed to cool to room temperature and the volume was reduced; a yellow-orange precipitate was formed and was collected on a frit, washed with ether and vacuum-dried. Yield: 144.9 mg (71.84 %). Anal. Found (Calc.) for C₁₀H₂₄Cl₂N₂O₃RuS₃: C, 24.61 (24.60); H, 4.94 (4.90); N, 5.69 (5.70). ¹H-NMR (CD₂Cl₂, 400MHz): δ 2.09 (s, 3H, H4), 3.12 (s, 6H, H6, H9), 3.40 (s, 6H, H5, H10), 3.45 (s, 6H, H7, H8), 7.48 (s, 1H, H1), 8.25 (s, 1H, H3), 13.71 (s, 1H, H2). ¹³C-NMR (CD₂Cl₂, 400 MHz): 9.3 (C4), 46.84 (C7, C8), 47.16 (C6, C9), 47.67 (C5, C10), 117.98 (C2), 129.37 (C1), 141.4 (C3). For the NMR assignments we use the same labelling scheme as for the X-ray structures (Figure 1). IR (ν, cm⁻¹): 3016, 2925, 1410, 1300, 1091, 1052, 1019, 676, 611. *E*_{pa} (CH₃CN +0.1M TBAH): 1.49V vs Ag/AgCl. UV-Vis (CH₂Cl₂) [*λ*_{max}, nm (ε, M⁻¹·cm⁻¹): 359 (573.8).

[Ru^{II}Cl₂(NO₂-pz-H)(dmsO-S)₃], 3. This compound was prepared following a method analogous to that described for **2** starting from compound *cis, fac*-[RuCl₂(dmsO-S)₃(dmsO-O)] (0.2g, 0.413 mmol) and 4-nitro-1H-pyrazole (0.046 g, 0.407 mmol). Yield: 122mg (56.89%). Anal. Found (Calc.) for C₉H₂₁Cl₂N₃O₅RuS₃: C, 20.7(20.8); H, 3.9(4.04); N, 7.9(8.1). ¹H-NMR (CD₂Cl₂, 400MHz): δ 3.20 (s, 6H, H5, H9), 3.45 (s, 6H, H4, H8), 3.47 (s, 6H, H6, H7), 8.38 (s, 1H, H1), 9.14 (s, 1H, H3), 15.1 (s, 1H, H2). ¹³C (CD₂Cl₂, 400MHz): δ 46.20 (C6, C7), 47.17 (C4, C8), 47.64 (C6, C7), 19.76 (C1), 139.33 (C3). IR (ν, cm⁻¹): 3150, 3024, 2915, 1515, 1405, 1335, 1108, 1039, 998, 819, 752, 672. *E*_{pa} (CH₃CN +0.1M TBAH): 1.60V vs Ag/AgCl. UV-Vis (CH₂Cl₂) [*λ*_{max}, nm (ε, M⁻¹·cm⁻¹): 310 (328.7).

[Ru^{II}Cl₂(CF₃-pz-H)(dmsO-S)₃], 4. This compound was prepared following a method analogous to that described for **2** starting from compound *cis, fac*-[RuCl₂(dmsO-S)₃(dmsO-O)] (0.1g, 0.2064 mmol) and 3-trifluoromethyl-pyrazole (0.028g, 0.206 mmol). Yield: 34.66mg (30.95%). Anal. Found (Calc.) C₁₀H₂₁Cl₂F₃N₂O₃RuS₃: C, 21.1(22.1); H, 3.3(3.8); N, 4.5(5.1). ¹H-NMR (CD₂Cl₂, 400MHz): δ 3.15 (s, 6H, H6, H10), 3.42 (s, 6H, H5, H9), 3.46 (s, 6H, H7, H8), 6.74 (s, 1H, H2A), 8.59 (s, 1H, H3), 15.33 (s, 1H, H2). ¹³C (CD₂Cl₂, 400MHz): δ 46.02 (C9, C10), 47.06 (C7, C8), 47.58 (C5, C6), 107.37 (C2), 134.67 (C1), 135.08 (C4), 143.7 (C3). IR (ν, cm⁻¹): 3115, 3010, 2925, 1458, 1350, 1318, 1100, 1014, 919, 794, 676. *E*_{pa} (CH₃CN +0.1M TBAH): 1.73V vs Ag/AgCl. UV-Vis (CH₂Cl₂) [*λ*_{max}, nm (ε, M⁻¹·cm⁻¹): 356 (560.34).

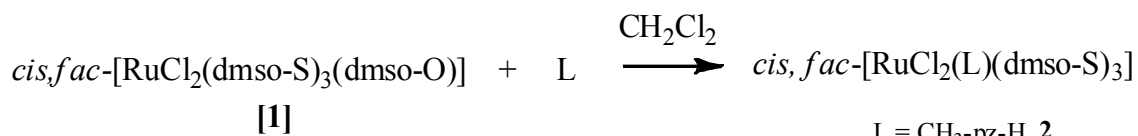
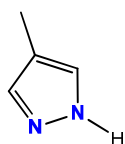
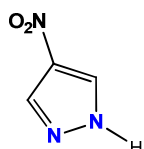
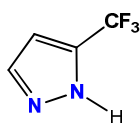
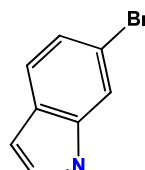
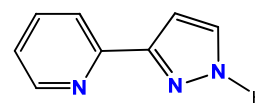
[Ru^{II}Cl₂(Br-Hind)(dmsO-S)₃], 5. This compound was prepared following a method analogous to that described for **2** starting from compound *cis, fac*-[RuCl₂(dmsO-S)₃(dmsO-O)] (0.2g, 0.4129 mmol) and 6-bromo-1H-indazole (0.081g, 0.412 mmol) except that the reflux was performed 20 min. Yield: 154.1mg (61.89 %) Anal. Found (Calc.) for C₁₃H₂₃BrCl₂N₂O₃RuS₃: C, 23.9 (25.1); H, 3.4 (3.8); N, 4.3 (4.04). ¹H-NMR (CD₂Cl₂, 400MHz): δ 3.17 (s, 6H, H9, H12), 3.45 (s, 6H, H8, H13), 3.49 (s, 6H, H10, H11), 7.30 (d, 1H, H4), 7.62 (s, 1H, H5), 7.76 (s, 1H, H2A), 9.11 (s, 1H, H7), 14.16 (s, 1H, H2B). ¹³C (CD₂Cl₂, 400MHz): δ 46.1 (C10, C11), 47.26 (C12, C13), 47.75 (C8, C9), 113.81 (C2), 122.10 (C6), 122.78 (C3), 123.3 (C5), 126.19 (C4), 139.03 (C7), 141.38 (C1). IR (ν, cm⁻¹): 3128, 3020, 2916, 2802, 1624, 1097, 1056, 1006, 950, 676, 590. E_{pa} (CH₃CN +0.1M TBAH): 1,66V vs Ag/AgCl. UV-Vis (CH₂Cl₂) [λ_{max}, nm (ε, M⁻¹·cm⁻¹): 343 (532.4).

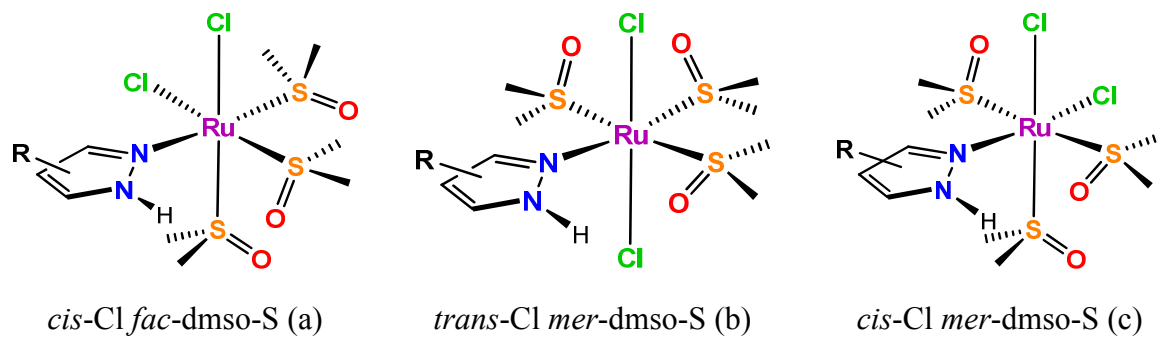
mer-[Ru^{III}Cl₃(pypz-H)(dmsO-S)], 6'. A 5 mg sample of **6** was dissolved in 10 ml of CHCl₃ and was irradiated overnight with light (80W tungsten lamp). The volume of the solution was reduced and a precipitate was formed after addition of Et₂O yielding complex **6'** in quantitative yield. Anal. Found (Calc.) for C₁₀H₁₃Cl₃N₃ORuS: C, 28.0 (27.8); H, 3.4 (3.0); N, 9.5 (9.7). E_{1/2} (CH₂Cl₂+0.1M TBAH): 0.05V vs Ag/AgCl. UV-Vis (CH₂Cl₂) [λ_{max}, nm (ε, M⁻¹·cm⁻¹): 276 (15112), 318 (5336), 360 (4464), 406 (9782).

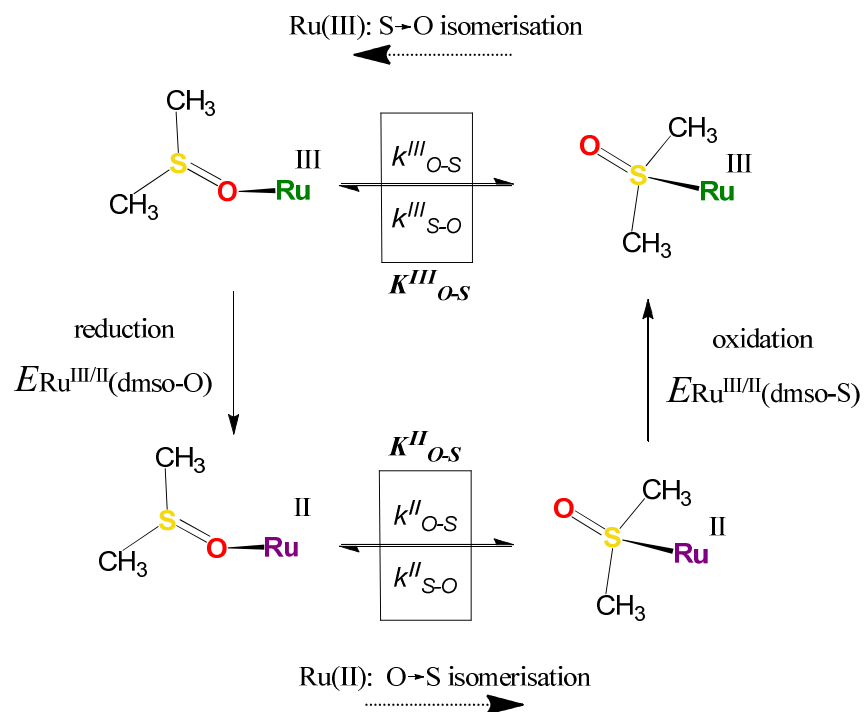
mer-[Ru^{III}Cl₃(CH₃-pz-H)(dmsO-S)₂], 2''. A 5 mg sample of **2** was dissolved in 10 ml of CHCl₃ and was irradiated overnight with light (80W tungsten lamp). The volume of the solution was reduced and a precipitate was formed after addition of Et₂O yielding complex **2''** in quantitative yield. E_{1/2} (CH₂Cl₂+0.1M TBAH): 0.1 V vs Ag/AgCl.

Acknowledgements

This research has been financed by MINECO of Spain (CTQ2010-21532-C02-01). IF thanks UdG for a predoctoral grant. Johnson & Matthey LTD are acknowledged for a RuCl₃·nH₂O loan.

Scheme 1. Synthetic strategy and ligands used in this work.L = CH₃-pz-H, **2**L = NO₂-pz-H, **3**L = CF₃-pz-H, **4**L = Br-Hind, **5****CH₃-pz-H****NO₂-pz-H****CF₃-pz-H****Br-Hind****pypz-H**

Scheme 2. Possible stereoisomers for complexes 2-5.

Scheme 3. Electron transfer and linkage isomerization processes observed for Ru-dmsO complexes.

Scheme 4. Photochemical transformation of complexes **2** and **6** in different solvents.

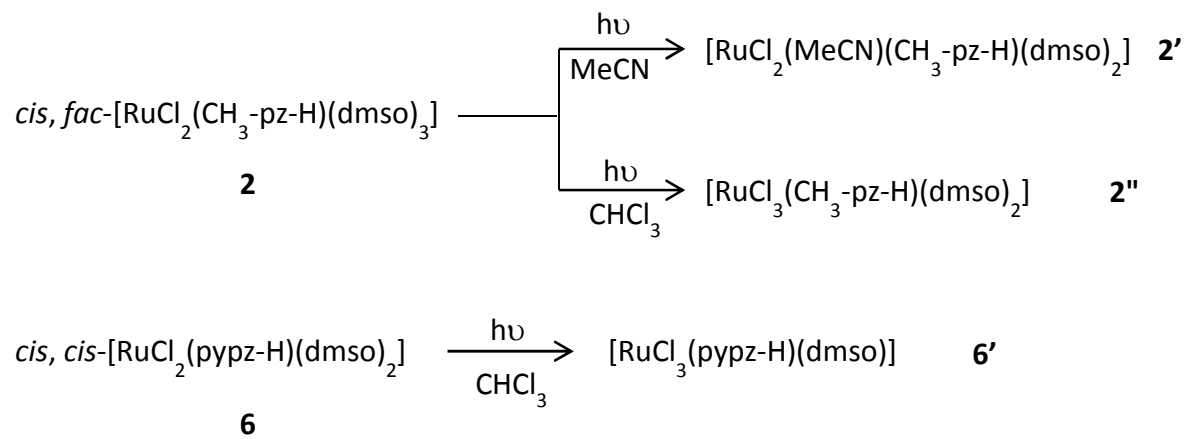


Table 1. Selected bond lengths (Å) and angles (°) for complexes **2-5** and **6'**

	2	3	4	5		6'
Ru(1)-N(1)	2.1461(18)	2.120(2)	2.145(3)	2.141(3)	Ru(1)-N(3)	2.019(3)
Ru(1)-S(1)	2.2682(7)	2.2455(15)	2.2817(10)	2.2780(15)	Ru(1)-N(1)	2.118(3)
Ru(1)-S(2)	2.3003(6)	2.2690(17)	2.2944(11)	2.2816(13)	Ru(1)-S(1)	2.2639(14)
Ru(1)-S(3)	2.2866(6)	2.2760(15)	2.2610(11)	2.2901(11)	Ru(1)-Cl(2)	2.3170(13)
Ru(1)-Cl(1)	2.4267(7)	2.4028(17)	2.3977(11)	2.4212(12)	Ru(1)-Cl(1)	2.3438(13)
Ru(1)-Cl(2)	2.1461(18)	2.3928(16)	2.4187(11)	2.4211(16)	Ru(1)-Cl(3)	2.3464(13)
N(1)-Ru(1)-S(1)	90.52(5)	88.82(5)	94.64(9)	92.63(9)	N(3)Ru(1)N(1)	77.91(12)
N(1)-Ru(1)-S(2)	171.03(5)	173.07(4)	172.82(9)	174.29(8)	N(3)Ru(1)S(1)	97.44(9)
N(1)-Ru(1)-S(3)	94.43(5)	94.80(5)	89.13(9)	88.35(9)	N(1)Ru(1)S(1)	174.81(9)
S(1)-Ru(1)-S(2)	96.14(2)	92.82(4)	91.91(4)	92.46(4)	N(3)Ru(1)Cl(2)	88.07(10)
S(1)-Ru(1)-S(3)	91.16(2)	93.48(6)	92.74(4)	90.25(5)	N(1)Ru(1)Cl(2)	86.27(9)
S(2)-Ru(1)-S(3)	91.44(2)	91.83(3)	93.48(4)	94.24(5)	S(1)Ru(1)Cl(2)	91.30(4)
N(1)-Ru(1)-Cl(1)	84.09(5)	85.69(5)	87.09(9)	85.53(9)	N(3)Ru(1)Cl(1)	86.28(10)
N(1)-Ru(1)-Cl(2)	88.02(5)	86.46(5)	85.49(9)	85.08(9)	N(1)Ru(1)Cl(1)	92.33(9)
S(1)-Ru(1)-Cl(1)	174.59(2)	174.487(19)	174.64(4)	87.12(5)	S(1)Ru(1)Cl(1)	89.66(4)
S(2)-Ru(1)-Cl(1)	89.17(2)	92.69(3)	87.35(4)	92.12(5)	Cl(2)Ru(1)Cl(1)	174.34(4)
S(3)-Ru(1)-Cl(1)	89.77(2)	86.52(6)	92.35(5)	173.22(4)	N(3)Ru(1)Cl(3)	172.46(9)
S(1)-Ru(1)-Cl(2)	90.79(2)	92.09(5)	87.35(4)	175.40(4)	N(1)Ru(1)Cl(3)	95.14(9)
S(2)-Ru(1)-Cl(2)	85.89(2)	86.76(3)	91.90(4)	89.67(4)	S(1)Ru(1)Cl(3)	89.62(4)
S(3)-Ru(1)-Cl(2)	176.86(2)	174.31(2)	174.61(4)	93.66(5)	Cl(2)Ru(1)Cl(3)	94.46(5)
Cl(1)-Ru(1)-Cl(2)	88.53(2)	88.05(6)	87.73(5)	88.73(5)	Cl(1)Ru(1)Cl(3)	91.12(5)

Table 2. Electrochemical data (CH₃CN +0.1M TBAP; *E* in V vs Ag/AgCl) for the complexes described in this work and others for purposes of comparison.

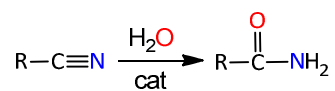
Compound	E_{pa} Ru ^{II} -S→Ru ^{III} -S	E_{pc} Ru ^{III} -O→Ru ^{II} -O
[RuCl ₂ (pz-H)(dmsO-S) ₃] ^a	1.60	0.82
[RuCl ₂ (CH ₃ -pz-H)(dmsO-S) ₃], 2	1.49	0.75
[RuCl ₂ (NO ₂ -pz-H)(dmsO-S) ₃], 3	1.62	0.86
[RuCl ₂ (CF ₃ -pz-H)(dmsO-S) ₃], 4	1.73	0.85
[RuCl ₂ (Br-Hind)(dmsO-S) ₃], 5	1.66	0.85
[RuCl ₂ (pypz-H)(dmsO-S) ₂], 6 ^a	1.09 ^b	0.33

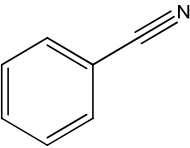
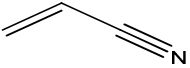
^a Reference 14 ^b $E_{1/2}$ value, in CH₂Cl₂ +0.1M TBAP

Table 3. Thermodynamic and kinetic parameters for the linkage isomerization in complexes **2** and **6**, together with related Ru-dmsO complexes.^a

Entry	Compound	K_{O-S}^{III}	k_{O-S}^{III} (s ⁻¹)	k_{S-O}^{III} (s ⁻¹)	K_{O-S}^{II}	k_{O-S}^{II} (s ⁻¹)	k_{S-O}^{II} (s ⁻¹)
1	<i>cis, fac</i> -[RuCl ₂ (CH ₃ -pz-H)(dmsO-S) ₃], 2	0.036	1.9·10 ⁻²	5.3·10 ⁻¹	1.53·10 ¹²	7.2·10 ⁻²	4.7·10 ⁻¹⁴
2	<i>cis, cis</i> -[RuCl ₂ (pypz-H)(dmsO-S) ₂], 6	1.39	1.76·10 ⁻¹	1.26·10 ⁻¹	1.34·10 ¹²	1.1·10 ⁻¹	8.2·10 ⁻¹⁴
3	<i>cis, cis</i> -[RuCl ₂ (H3p)(dmsO-S) ₂] (ref 19)	1.7	2.8·10 ⁻¹	1.7·10 ⁻¹	5.2·10 ¹¹	4.9·10 ⁻¹	9.3·10 ⁻¹⁴
4	<i>trans, cis</i> -[RuCl ₂ (H3p)(dmsO-S) ₂] (ref 19)	0.27	5.7·10 ⁻²	2.2·10 ⁻¹	5.3·10 ⁸	8.7·10 ⁻²	1.6·10 ⁻¹⁰
5	<i>trans, cis</i> -[RuCl ₂ (bpp)(dmsO-S) ₂] ⁻ (ref 3)	0.26	1.7·10 ⁻²	6.5·10 ⁻²	6.5·10 ⁹	1.3·10 ⁻¹	2.1·10 ⁻¹¹
6	<i>out</i> -[Ru(L ²)(trpy)(dmsO-S)] ⁺ (ref 5)	0.13	7.7·10 ⁻²	6.0·10 ⁻¹	5.5·10 ⁸	2.5·10 ⁻¹	4.6·10 ⁻¹⁰

^aH3p is 5-phenyl-3-(2-pyridyl)-1*H*-pyrazole, L² is 5-phenyl-3-(pyridin-2-yl)pyrazolate and bpp is 3,5-(2-pyridyl)pyrazolate (see Scheme S1 in the supplementary information for a schematic drawing of the complexes)

Table 4. Ru-catalyzed hydration of nitriles to amides in water using complexes **2-6** as catalysts.^a

Substrate	Cat.	Yield [%]	Select.(%) ^b
	[RuCl ₂ (pz-H)(dmsO-S) ₃] ^c	80 ^c	>99 ^c
	2	29	>99
	3	85	>99
	4	24	>99
	5	30	>99
	6	70	>99
		[RuCl ₂ (pz-H)(dmsO-S) ₃] ^c	61 ^c
	2	35	>99
	3	40	>99
	4	53(30) ^d	>99
	5	43	>99
	6	22	>99

^a Reactions performed at 80°C using 1 mmol of nitrile in 3ml of water.

[Substrate]:[Ru] ratio = 100:1. Time: 20 h reaction

^b Selectivity = (amide yield/substrate conversion) x 100^c reference 14^d In parentheses, reaction performed at 50°C

Figure Captions

Figure 1. Ortep plots and labelling schemes for compounds **2-5**.

Figure 2. Cyclic voltammeteries of complex **2** recorded in CH₃CN: solid line, potential scan starting at $E_{\text{init}} = 0$ V with 2 s equilibrium time; dashed line, potential scan starting at $E_{\text{init}} = 1.8$ V with 10 min equilibrium time.

Figure 3. CV registered in CH₂Cl₂ (TBAH, 0.1M) vs Ag/AgCl starting the scanning potential at $E_{\text{init}} = 1.7$ V for **2** and 1.4 V for **6**, at scan rates between 0.20 and 8 V/s and applying an equilibration time of 1 minute. a) complex **2**, b) complex **6**.

Figure 4. UV-visible spectra corresponding to the photochemical transformation of **2** into **2'** upon light irradiation in acetonitrile.

Figure 5 . Ortep plot and labelling schemes for the X-ray structure of compound **6'**.

Figure 6. DPV of a solution of complex **2''** in CH₂Cl₂ + 0.1M TBAP, starting the scanning of potential at a) -0.2 V and b) 0.6 V. The equilibrium time applied in each case (0-180 s) is indicated.

Figure 1.

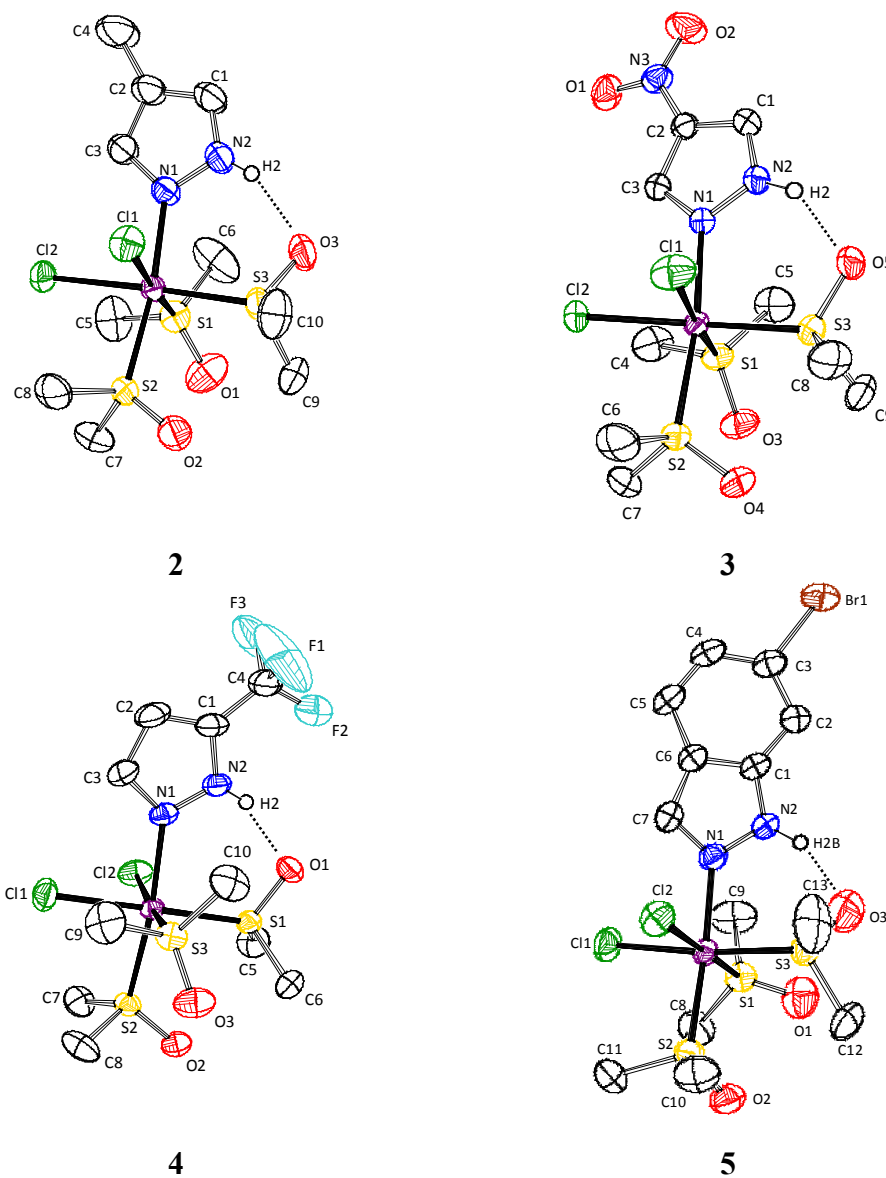


Figure 2.

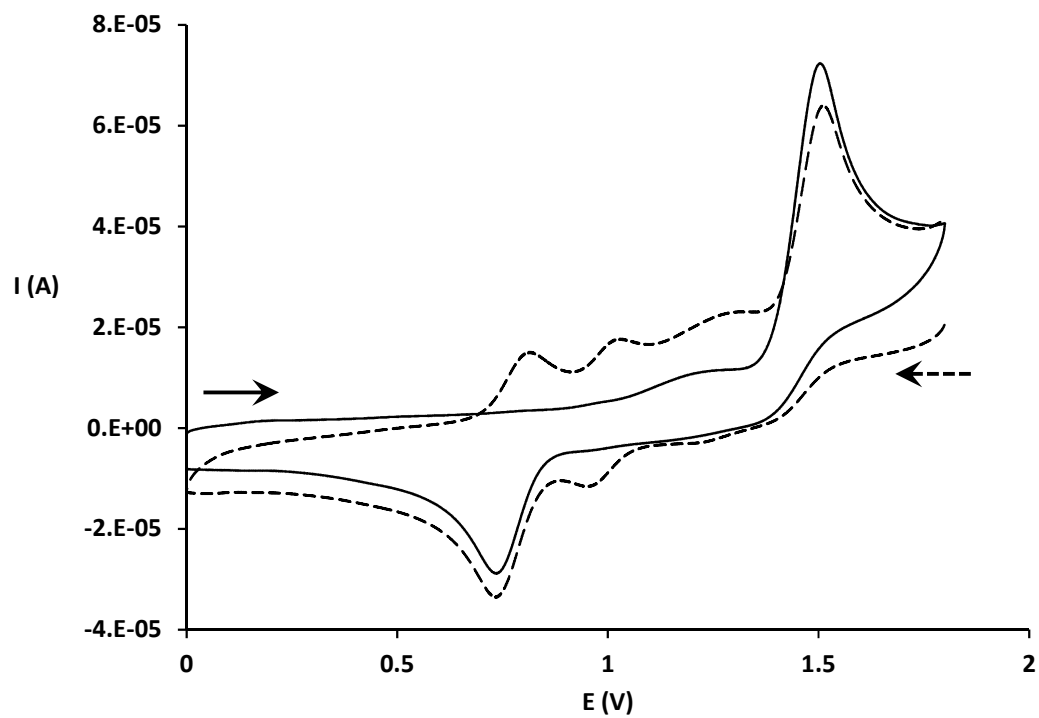


Figure 3.

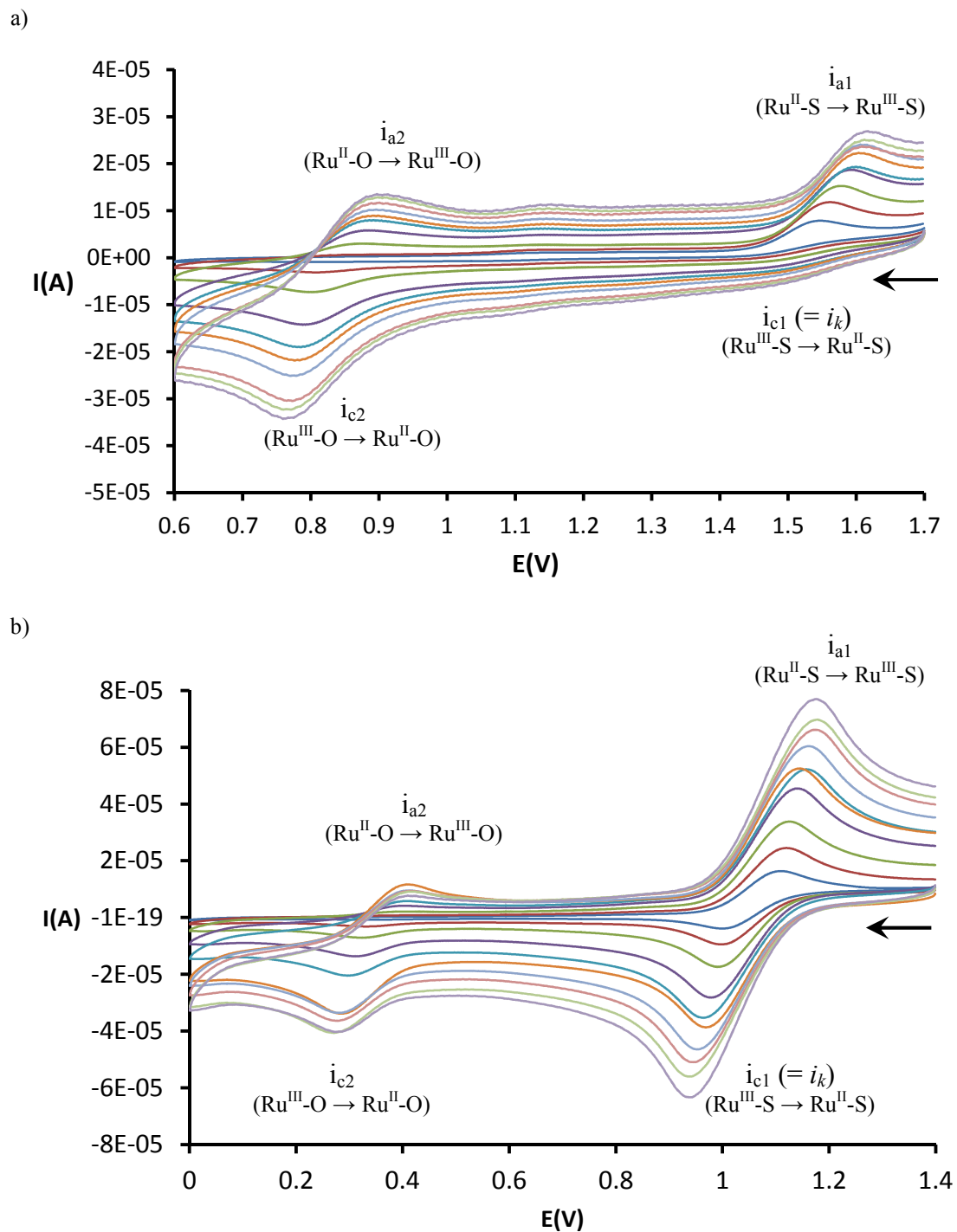


Figure 4.

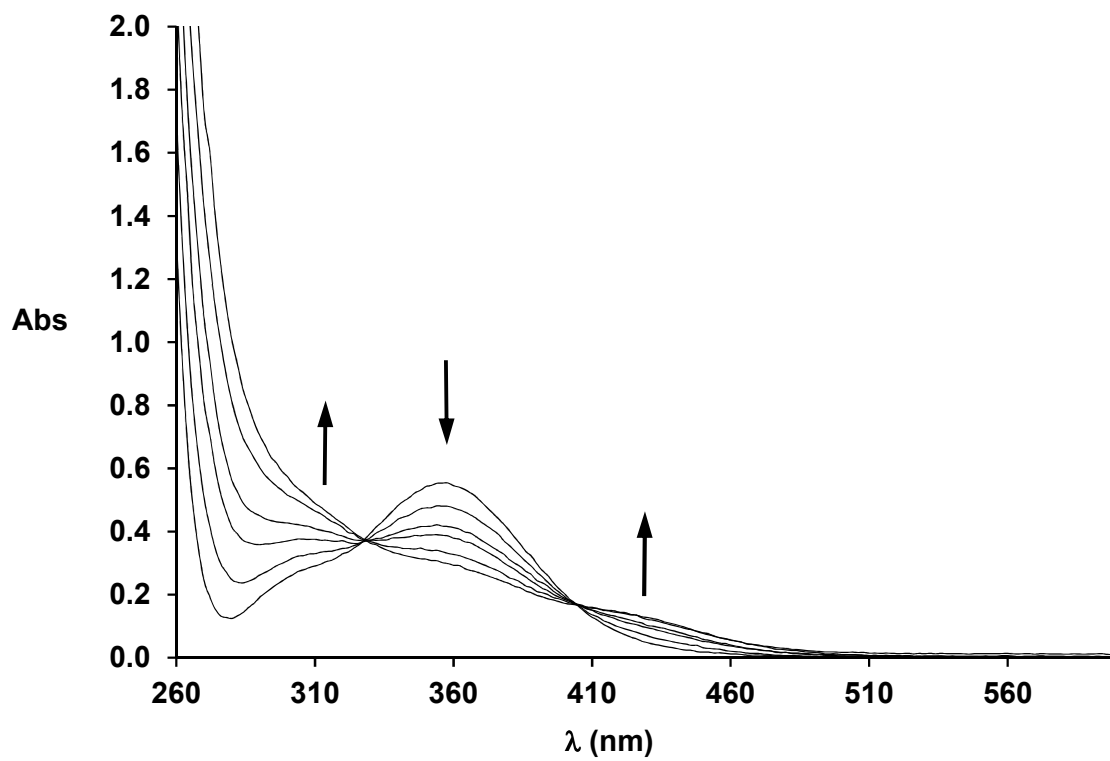


Figure 5.

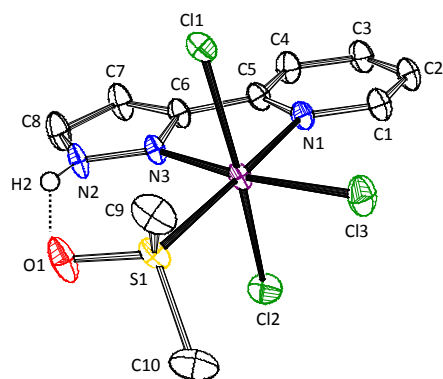
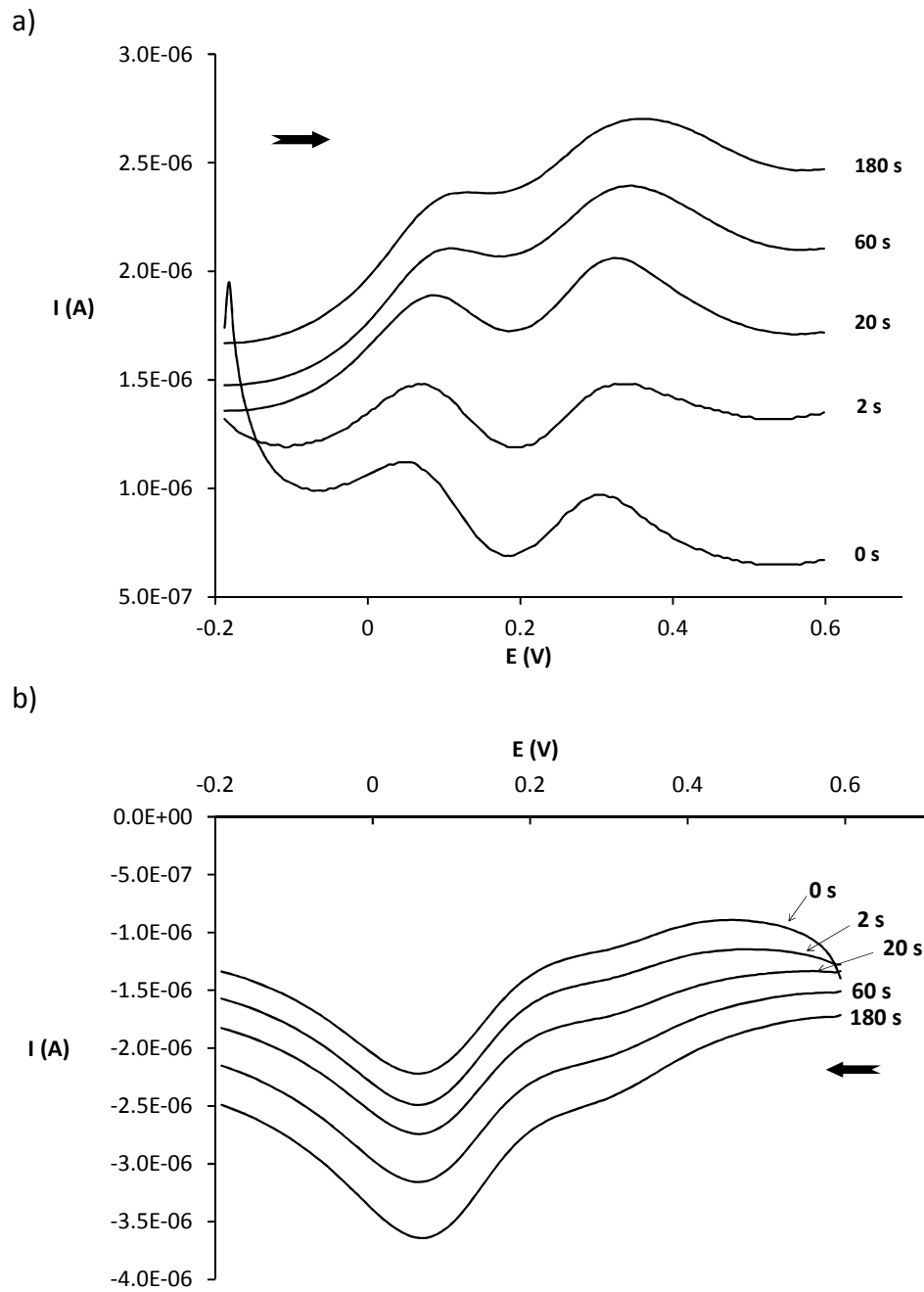


Figure 6.



REFERENCES

1 (a) G. Sava, E. Alessio, A. Bergamo and G. Mestroni, *Topics in Biological Inorganic Chemistry*, Springer-Verlag GmbH & Co., Berlin, 1999; (b) G. Sava, Clerici, I. Capozzi, M. Cocchietto, R. Gagliardi, E. Alessio, G. Mestroni and A. Perbellini, *Anticancer. Drugs*, 1999, **10**, 129–138; (c) G. Sava, R. Gagliardi, A. Bergamo, E. Alessio and G. Mestroni, *Anticancer Res.*, 1999, **19**, 969–972; (d) I. Bratsos, D. Urankar, E. Zangrando, P. Genova-Kalou, J. Košmrlj, E. Alessio and I. Turel, *Dalton Trans.*, 2011, **40**, 5188–5199.

2 (a) I. P. Evans, A. Spencer and G. Wilkinson, *J. Chem. Soc., Dalton Trans.*, 2, 204–209; (b) E. Alessio, G. Mestroni, G. Nardin, W. M. Attia, M. Calligaris, G. Sava and S. Zorzet, *Inorg. Chem.*, 1988, **27**, 4099–4106; (c) I. Bratsos and E. Alessio, in *Inorganic Synthesis*, ed. T. B. Rauchfuss, John Wiley & Sons, Inc., Hoboken, NJ, USA, 2010, vol. 35, pp. 148–152; (d) E. Alessio, *Chem. Rev.*, 2004, **104**, 4203–42; (e) J. Mola, I. Romero, M. Rodríguez, F. Bozoglian, A. Poater, M. Solà, T. Parella, J. Benet-Buchholz, X. Fontrodona and A. Llobet, *Inorg. Chem.*, 2007, **46**, 10707–10716.

3 C. Sens, M. Rodríguez, I. Romero, A. Llobet, T. Parella, B. P. Sullivan and J. Benet-Buchholz, *Inorg. Chem.*, 2003, **42**, 2040–8.

4 A. M. Khenkin, L. J. W. Shimon and R. Neumann, *Inorg. Chem.*, 2003, **42**, 3331–9.

5 J. Benet-Buchholz, P. Comba, A. Llobet, S. Roeser, P. Vadivelu and S. Wiesner, *Dalton Trans.*, 2010, **39**, 3315–3320.

6 (a) N. N. Dass and S. R. Sen, *J. Polym. Sci. Polym. Chem. Ed.*, 1983, **21**, 3381–3388; (b) R. Castarlenas, I. Alaoui-Abdallaoui, D. Sémeril, B. Mernari, S. Guesmi and P. H. Dixneuf, *New J. Chem.*, 2003, **27**, 6–8.

7 N. V. Kaminskaia and N. M. Kostic, *J. Chem. Soc. Dalton Trans.*, 1996, 3677–3686.

8 (a) P. Lugo-Mas, A. Dey, L. Xu, S. D. Davin, J. Benedict, W. Kaminsky, K. O. Hodgson, B. Hedman, E. I. Solomon and J. A. Kovacs, *J. Am. Chem. Soc.*, 2006, **128**, 11211–21; (b) J. A. Kovacs, *Chem. Rev.*, 2004, **104**, 825–48.

9 (a) H. Yamada and M. Kobayashi, *Biosci Biotechnol Biochem*, 1996, **60**, 1391–1400; (b) I. Endo, M. Nojiri, M. Tsujimura, M. Nakasako, S. Nagashima, M. Yohda and M. Odaka, *J. Inorg. Biochem.*, 2001, **83**, 247–253; (c) S. Sanchez and A. L. Demain, *Org. Process Res. Dev.*, 2011, **15**, 224–230; (d) B. Li, J. Su and J. Tao, *Org. Process Res. Dev.*, 2011, **15**, 291–293.

10 (a) J. Zabicky, *The chemistry of amides*, Interscience publishers, John Wiley & Sons Ltd., London, 1970; (b) A. Greenberg, C. M. Breneman and J. F. Liebman, *The Amide Linkage: Structural Significance in Chemistry, Biochemistry, and Materials Science*, Wiley-Interscience, 2000.

11 A. Bhattacharya, B. P. Scott, N. Nasser, H. Ao, M. P. Maher, A. E. Dubin, D. M. Swanson, N. P. Shankley, A. D. Wickenden and S. R. Chaplan, *J. Pharmacol. Exp. Ther.*, 2007, **323**, 665–674.

12 T. J. Ahmed, S. M. M. Knapp and D. R. Tyler, *Coord. Chem. Rev.*, 2011, **255**, 949–974.

13 (a) V. Cadierno, J. Francos and J. Gimeno, *Chem. Eur. J.*, 2008, **14**, 6601–5; (b) V. Cadierno, J. Díez, J. Francos and J. Gimeno, *Chem. Eur. J.*, 2010, **16**, 9808–17; (c) A. Cavarzan, A. Scarso and G. Strukul, *Green Chem.*, 2010, **12**, 790–794; (d) R. García-Álvarez, J. Díez, P. Crochet and V. Cadierno, *Organometallics*, 2010, **29**, 3955–3965; (e) R. García-Álvarez, J. Díez, P. Crochet and V. Cadierno, *Organometallics*, 2011, **30**, 5442–5451; (f) R. García-Álvarez, P. Crochet and V. Cadierno, *Green Chem.*, 2013, **15**, 46–66.

14 Í. Ferrer, J. Rich, X. Fontrodona, M. Rodríguez and I. Romero, *Dalton Trans.*, 2013, **42**, 13461–9.

15 (a) M. M. R. Choudhuri and R. J. Crutchley, *Inorg. Chem.*, 2013, **52**, 14404–10; (b) J. J. Rack, J. R. Winkler and H. B. Gray, *J. Am. Chem. Soc.*, 2001, **123**, 2432–2433; (c) A. A. Rachford, J. L. Petersen and J. J. Rack, *Inorg. Chem.*, 2005, **44**, 8065–75; (d) M. Sano and H. Taube, *Inorg. Chem.*, 1994, **33**, 705–709.

16 H. Dong, H. Zhu, Q. Meng, X. Gong and W. Hu, *Chem. Soc. Rev.*, 2012, **41**, 1754–808.

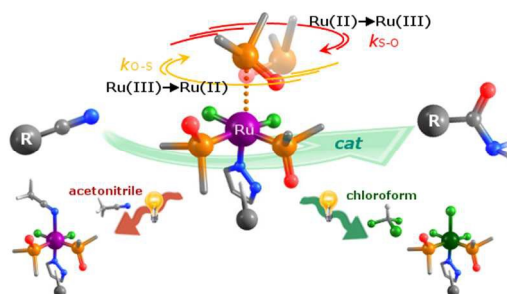
17 S. Bonnet, J.-P. Collin, M. Koizumi, P. Mobian and J.-P. Sauvage, *Adv. Mater.*, 2006, **18**, 1239–1250.

18 J. J. Rack, *Coord. Chem. Rev.*, 2009, **253**, 78–85.

19 S. Roeser, S. Maji, J. Benet-Buchholz, J. Pons and A. Llobet, *Eur. J. Inorg. Chem.*, 2013, **2013**, 232–240.

- 20 V. Balzani, A. Juris, M. Venturi, S. Campagna and S. Serroni, *Chem. Rev.*, 1996, **96**, 759–834.
- 21 R. S. Nicholson and I. Shain, *Anal. Chem.*, 1964, **36**, 706–723.
- 22 D. O. Silva and H. E. Toma, *Can. J. Chem.*, 1994, **72**, 1705–1708.
- 23 L. R. Cohen, L. A. Peña, A. J. Seidl, K. N. Chau, B. C. Keck, P. L. Feng and P. E. Hoggard, *J. Coord. Chem.*, 2009, **62**, 1743–1753.
- 24 A. Gerli, J. Reedijk, M. T. Lakin and A. L. Spek, *Inorg. Chem.*, 1995, **34**, 1836–1843.
- 25 F. Weisser, S. Hohloch, S. Plebst, D. Schweinfurth and B. Sarkar, *Chem. Eur. J.*, 2014, **20**, 614–614.
- 26 J. J. Rack and H. B. Gray, *Inorg. Chem.*, 1999, **38**, 2–3.
- 27 (a) N. E. Katz, F. Fagalde, N. D. Lis de Katz, M. G. Mellace, I. Romero, A. Llobet and J. Benet-Buchholz, *Eur. J. Inorg. Chem.*, 2005, **2005**, 3019–3023; (b) J. Mola, D. Pujol, M. Rodríguez, I. Romero, X. Sala, N. Katz, T. Parella, J. Benet-Buchholz, X. Fontrodona and A. Llobet, *Aust. J. Chem.*, 2009, **62**, 1675–1683.

Table of contents entry



Photochemical ligand substitution in acetonitrile and chloroform, together with the kinetics of dmsoligand isomerization, are investigated on new Ru(II)-dmsoligand complexes that are also active as nitrile hydration catalysts.